Eur Radiol (2009) 19: 1366–1378
DOI 10.1007/s00330-008-1289-y

GASTROINTESTINAL

G. P. Schmidt
A. Baur-Melnyk
A. Haug
S. Utzschneider
C. R. Becker
R. Tiling
M. F. Reiser
K. A. Hermann

Whole-body MRI at 1.5 T and 3 T compared with FDG-PET-CT for the detection of tumour recurrence in patients with colorectal cancer

Received: 2 August 2008
Accepted: 9 December 2008
Published online: 4 February 2009

G. P. Schmidt (✉) · A. Baur-Melnyk · C. R. Becker · M. F. Reiser · K. A. Hermann
Department of Clinical Radiology, University Hospitals Grosshadern, Ludwig Maximilian University Munich,
Marchioninistr. 15,
81377 Munich, Germany
e-mail: gerwin.schmidt@med.uni-muenchen.de
Tel.: +49-89-70950
Fax: +49-89-70958832

A. Haug · R. Tiling
Department of Nuclear Medicine, University Hospitals Grosshadern, Ludwig Maximilian University Munich,
Marchioninistr. 15,
81377 Munich, Germany

S. Utzschneider
Department of Orthopedics, University Hospitals Grosshadern, Ludwig Maximilian University Munich,
Marchioninistr. 15,
81377 Munich, Germany

Abstract The purpose of this study was to assess the diagnostic accuracy of whole-body MRI (WB-MRI) at 1.5 T or 3 T compared with FDG-PET-CT in the follow-up of patients suffering from colorectal cancer. In a retrospective study, 24 patients with a history of colorectal cancer and suspected tumour recurrence underwent FDG-PET-CT and WB-MRI with the use of parallel imaging (PAT) for follow-up. High resolution coronal T1w-TSE and STIR sequences at four body levels, HASTE imaging of the lungs, contrast-enhanced T1w- and T2w-TSE sequences of the liver, brain, abdomen and pelvis were performed, using WB-MRI at either 1.5 T (n=14) or 3 T (n=10). Presence of local recurrent tumour, lymph node involvement and distant metastatic disease was confirmed using radiological follow-up within at least 5 months as a standard of reference. Seventy seven malignant foci in 17 of 24 patients (71%) were detected with both WB-MRI and PET-CT. Both investigations concordantly revealed two local recurrent tumours. PET-CT detected significantly more lymph node metastases (sensitivity 93%, n=27/29) than WB-MRI (sensitivity 63%, n=18/29). PET-CT and WB-MRI achieved a similar sensitivity for the detection of organ metastases with 80% and 78%, respectively (37/46 and 36/46). WB-MRI detected brain metastases in one patient. One false-positive local tumour recurrence was indicated by PET-CT. Overall diagnostic accuracy for PET-CT was 91% (sensitivity 86%, specificity 96%) and 83% for WB-MRI (sensitivity 72%, specificity 93%), respectively. Examination time for WB-MRI at 1.5 T and 3 T was 52 min and 43 min, respectively; examination time for PET-CT was 103 min. Initial results suggest that differences in accuracy for local and distant metastases detection using FDG-PET-CT and WB-MRI for integrated screening of tumour recurrence in colorectal cancer depend on the location of the malignant focus. Our results show that nodal disease is better detected using PET-CT, whereas organ disease is depicted equally well by both investigations.

Keywords Colorectal cancer · Magnetic resonance imaging · Computed tomography · Positron emission tomography

Introduction

Colorectal cancer is the third most common form of cancer and second leading cause of cancer-related death in the Western world resulting in 655,000 deaths worldwide per year [1]. Approximately 40% of patients treated with a curative approach will develop recurrent cancer within the first 3 years, for the most part manifesting as metastatic disease [2, 3]. Yet, compared with other malignancies, both local recurrence and metastatic spread from colorectal cancer can be addressed by curative-intent surgery or intervention [4–6]. Therefore, early diagnosis and accu-

rate restaging of recurrent colorectal cancer is important to define appropriate therapeutic strategies or to identify patients with limited disease who potentially could benefit from curative approaches. Follow-up of colorectal cancer usually is performed with multiple imaging techniques, including computed tomography (CT), magnetic resonance imaging (MRI), radiographs or ultrasound, the standard routine assessment being CT of the thorax and abdomen for regular restaging of the disease. However, a sequential imaging approach can be time-intensive and potential false-negative findings may delay appropriate therapy.

The introduction of combined PET-CT has expanded diagnostic options as the functional information of a PET exam is added to the detailed anatomical data of CT within a single examination. It has been reported that PET-CT has markedly increased lesion localization and diagnostic accuracy compared with either investigation alone [7, 8]. Recent studies indicate the clinical value of PET-CT in staging of colorectal cancer with an improved diagnostic accuracy and relevant impact on therapy [9–11].

MRI, with its lack of ionizing radiation, high soft tissue contrast and spatial resolution is a useful application for tumour detection and staging of malignant disease. A high sensitivity has been reported for the detection of organ metastases, especially for tumours frequently metastasizing to the liver, bone or the brain, like colorectal cancer [12–14]. However, different requirements in coil setup, sequence design and slice positioning as well as time-consuming patient repositioning procedures in the past have delayed the realization of WB-MRI as a clinical application. With the introduction of multichannel whole-body scanners, MRI has become a promising candidate for whole-body tumour imaging. Now, dedicated assessment of individual organs with various soft tissue contrast, image orientation, spatial resolution and contrast media dynamics can be combined with whole-body anatomic coverage [15, 16].

Recently, approved clinical multichannel whole-body MR systems with a field strength of 3 T became available. The potential twofold gain in SNR at 3 T can be used for either acquisition acceleration or increased spatial resolution, or for a compromise of both, resulting in even shorter total examinations times, increased patient comfort and acceptance. Very few scientific studies have described the use of high-field systems in other parts of the body, including the chest and abdomen, or in whole-body applications [17, 18].

The purpose of this study was to compare the diagnostic potential of FDG-PET-CT and WB-MRI at 1.5 T and 3 T in patients with colorectal cancer and suspected tumour recurrence.

Materials and methods

The study included 24 patients (mean age 62 years, range 47–80 years) with a history of colorectal cancer, all treated with a primarily curative approach. The patients were referred to our hospital within a time period of 33 months for follow-up with either suspected tumour recurrence (n= 10) or a conspicuous finding in another imaging modality (n=14). All patients were examined consecutively with a dual-modality PET-CT system (Gemini, Philips Medical Systems, Cleveland, Ohio) within the diagnostic algorithms of clinical routine. The patients also underwent WB-MRI at 1.5 T or 3 T within a mean period of 3 days (maximum interval 12 days). MRI was performed in agreement with the patients as well as the clinicians in charge. Approval of the institutional review board and written patient consent were obtained beforehand. Both PET-CT and WB-MRI (irrespective of the applied field strength) were well tolerated by all patients. No iodine-based contrast agent was administered during the PET-CT examination of one patient who refused contrast media administration. To avoid bias in diagnostic accuracy of PET-CT due to suppressed metabolic activity, patients receiving chemotherapy/radiotherapy immediately before or between our examinations were excluded from statistical analysis.

Whole-body MRI at 1.5 T

In 14 patients WB-MRI was performed on a 1.5-T (40 mT min^{-1}, max. slew rate 20 T m^{-1} s^{-1}) whole-body MR system (Magnetom Avanto, Siemens Medical Solutions, Erlangen, Germany). Using the integrated body matrix receiver coil system and automated table motion, parallel acquisition techniques in three spatial directions at a maximum imaging range of 205 cm were performed without patient repositioning. The patients were examined from head to the proximal calves with STIR sequences on four body levels in coronal orientation: head/neck, pelvis, thighs/calves (TR 5,620/TE 92), as well as the thorax/abdomen (TR 3,380/TE 101) in breath-hold technique with prospective 2D-navigator correction (PACE, prospective acquisition correction). Subsequently, the body was examined with coronal T1-weighted TSE imaging (TR 79/TE 12; thorax/abdomen TR 400/TE 8.2, breath-hold technique). The lung was examined in axial orientation with STIR (TR 3,800/TE 100) and HASTE sequences (TR 1,100/TE 27), followed by a respiratory-triggered T2w fat saturated TSE exam of the liver (TR 2,010/TE 101) and coronal HASTE of the abdomen (TR 900,TE 73). Then, sagittal imaging of the upper and lower spine with T1-weighted TSE (TR 849/TE11) and STIR sequences (TR 5,700/TE 59) was performed.

After intravenous application of gadolinium-DTPA (Magnevist®, Bayer Schering Pharma, Berlin, Germany, 3 mL s^{-1}; 0.2 mmol kg^{-1}, 20 mL saline flushing), a dynamic (arterial, portal venous, late venous phase) axial 3D-VIBE (volume interpolated breath-hold exam) liver exam was accomplished (TR 4.38/TE 1.61) including a late venous MR acquisition of the lung level (TR 9.1/TE 4.76). Axial T1w- and T2w-TSE imaging (TR 635/TE 17 and TR 1,420/TE 109) of the brain was then performed. Finally, a fat saturated T1w-GRE sequence of the whole abdomen in axial orientation (TR 179/TE 3.33) was performed. Table 1 gives an overview of the applied examination protocol.

Whole-body MRI at 3 T

In 10 patients WB-MRI was performed on a 3 T (40 mT min^{-1}, max. slew rate 20 T m^{-1} s^{-1}) MR system (Magnetom Tim Trio, Siemens Medical Solutions, Erlangen, Germany). During migration of the described established protocol at 1.5 T to higher field conditions, adaptions of imaging parameters to the different field strength were performed. No further adjustments or optimizations (such as spatial resolution) were made to preserve comparability of the two protocols (see Table 1).

Accordingly, coronal STIR (TR 5,900/TE 100/TI 200; thorax/abdomen TR 3,830/TE 117) and T1w-TSE-WB-MRI (TR 750/TE 9.6 and TR 700/TE 9.1) were performed, including sagittal imaging of the spine, HASTE of the lung (TR 531/TE 33)/abdomen (TR 1,100/TE 111) as well as the T2w-TSE exam of the liver (TR 3,500/ TE 81). As a result of changed relaxation times for STIR imaging, T1 was increased to 200 ms (cf. 170 ms at 1.5 T) to achieve an adequate fat suppressed bone marrow signal. For the head/neck region SE imaging (TR 800/TE 9) was used to achieve adequate image contrast and detail for brain parenchyma and soft tissue structures of the neck/shoulder. As a result of increased SAR at 3 T, a pulse technique with variable rate selective excitation (VERSE) was selected for T1-weighted TSE and STIR imaging allowing substantial SAR reduction without significant increase of TR and at negligible changes of image contrast [19]. Compared with the 1.5-T protocol, a T1-weighted Flash-2D GRE sequence (TR 471/TE 4.9) was applied as established T1w brain imaging of choice with high CNR and robust image quality at higher field strength [20].

Contrast-enhanced 3D-VIBE imaging of the liver (TR 2.96 /TE 1.17), a late venous MR acquisition of the lung (TR 2.85 /TE 1.07) and fat saturated GRE sequence on the abdomen/pelvis (TR 189 /TE 3.69) were performed. Additionally, a dielectric pad was placed on patients with low body fat to avoid dielectric artefacts [21]. Axial STIR imaging of the lung was not applied due to severe impairment of image quality from pulsation artefacts.

Table 1 WB-MRI protocol for oncologic imaging on a 32-receiver channel whole-body MR system at 1.5 T or 3 T

Sequence	Image plane	Matrix	Resolution (mm^2)	Slice (mm)	Gap (%)	1.5 T Acq. time (min)	3 T Acq. time (min)
STIR-WB	Coronal	384	1.8×1.3	5.0	10	9:43	6:40
HASTE abdo	Coronal	384	1.4×1.3	5.0		0:38	0:33
HASTE lung	Axial	320	1.3×1.2	6.0		0:44	0:42
(STIR lung)[a]	(Axial)	(320)	1.8×1.2	6.0		(1:01)	–
T2w fs TSE liver (free breathing)	Axial	320	1.6×1.2	5.0		3:41	3:41
T1w TSE-WB[b]	Coronal	384	1.7×1.3	5.0		10:30	7:53
T1w TSE spine	Sagittal	384	1.0×1.0	3.0		7:46	6:15
STIR spine	Sagittal	384	1.0×1.0	3.0		7:22	7:00
Dyn. VIBE liver	Axial	384	1.9×1.5	3.0		2:20	2:20
Stat. VIBE thorax[a]	Axial	380	1.6×1.6	1.5		0:25	0:25
T1w fs GRE pelvis	Axial	320	1.5×1.2	6.0		1:17	1:10
T1w TSE brain	Axial	320	0.7×0.7	5.0		3:11	–
T1w GRE brain[c]	Axial					–	3:17
T2w TSE brain	Axial	512	0.5×0.5	5.0		3:11	2:52
Total						51:49	42:48

[a]At 3 T axial STIR imaging of the lung was not performed due to severe pulsation artefacts
[b]At 3 T alternatively an SE sequence was applied for coronal imaging of the head/neck region
[c]At 3 T T1-weighted axial imaging of the brain was performed with a Flash-2D gradient echo sequence. Total imaging time is 52 min at 1.5 T and 43 min at 3 T with unchanged image resolution

FDG-PET-CT imaging

Examinations were performed on a two-detector row PET-CT system (Gemini, Philips Medical Systems, Cleveland, Ohio). Patients were asked to fast for at least 6 h before examination to assure blood glucose levels below 150 mg dL^{-1}. Buscopan was applied intravenously to avoid a first-pass uptake of FDG into smooth muscle, and 20 mg of furosemide was given to increase renal excretion of the tracer. One hour after FDG administration a low-dose CT acquisition in shallow breathing was performed for PET attenuation correction covering neck, thorax, abdomen and pelvis (see Table 2). The emission PET acquisition followed using a 3D-RAMLA (row action maximum

Table 2 Whole-body protocol for FDG-PET-CT imaging on a two-detector row PET-CT system using an initial low-dose CT for attenuation correction

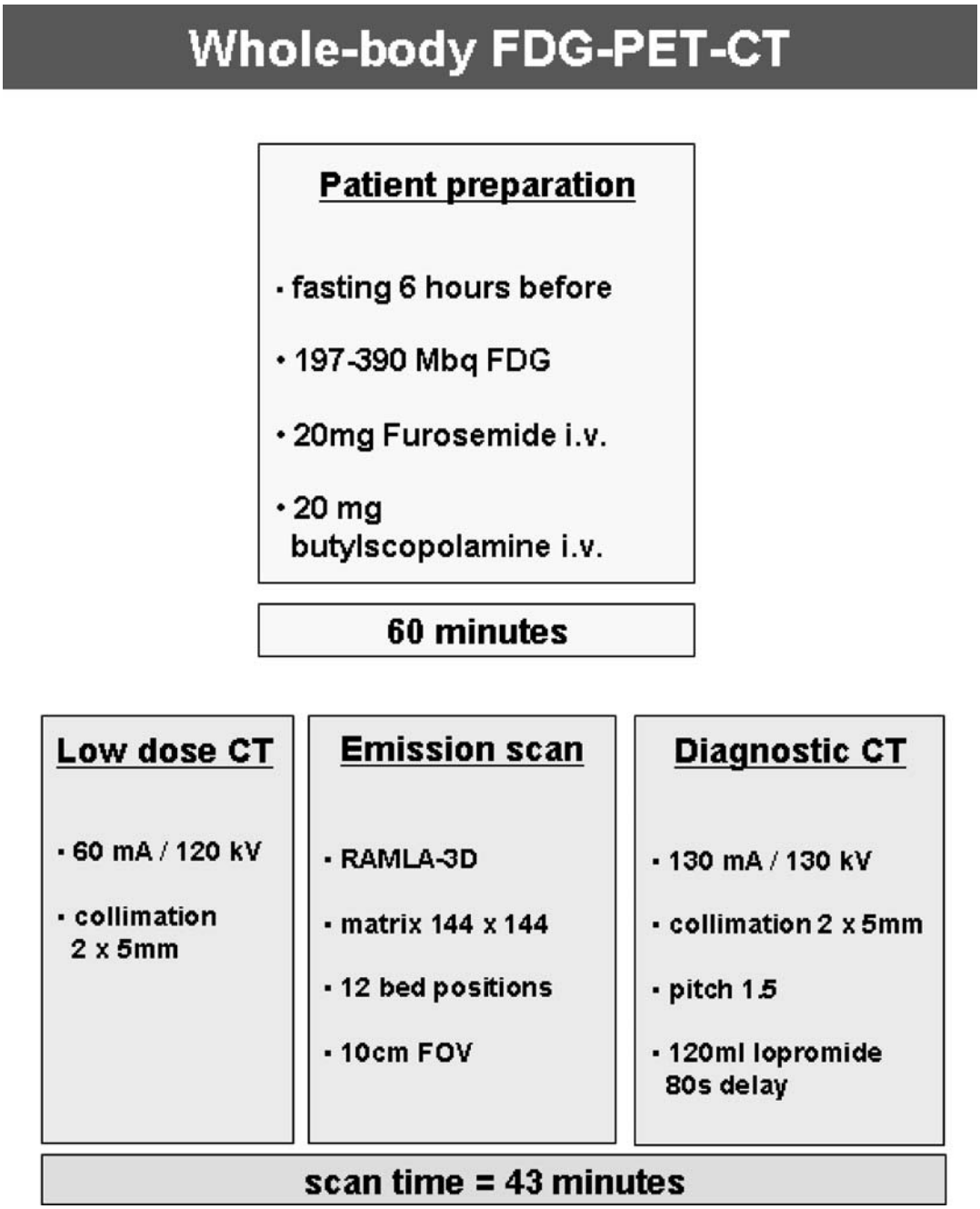

likelihood) algorithm for reconstruction. Finally, a diagnostic contrast-enhanced CT was conducted following i.v. administration of 120 mL contrast agent (Ultravist® 300, Bayer Schering Pharma, Berlin, Germany) in the venous phase (80-s delay). The PET and diagnostic CT data were fused with the use of special software (Syntegra®, Philips Medical Systems, Cleveland, Ohio). For the whole examination an average dose of ionizing radiation of 25 mSV has been calculated [22].

Data analysis

Two board-certified radiologists, each with more than 6 years of experience, read the MRI examinations and another radiologist and one nuclear medicine physician with 3 and 6 years of experience read the PET-CT images, each in consensus. Both reader groups were fully blinded to the other investigation and had no information on previous or current diagnostic imaging results.

Location, extension and number of suspected malignant lesions were recorded. Established region-specific size criteria were applied to determine tumour involvement when assessing lymph nodes, besides other morphologic criteria such as loss of hilar fat and rounded aspect of a node. Hard criteria for malignancy in both investigations were signs of aggressive expansion of a lesion, like ill-defined borders, erosion or infiltration of neighbouring anatomical structures, haemorrhage or signs of necrosis. In MRI, malignancy was determined based on established sequence-specific signal changes, e.g. a hypointense bone marrow signal in T1-weighted imaging in combination with a hyperintense signal in STIR in the case of bone lesions [23]. Furthermore, classic findings of abnormal static (CT) or dynamic (MRI) contrast uptake characteristics were consulted, like an early ring enhancement in the case of a malignant liver lesion [24]. In addition, malignancy in PET-CT was defined by a focally increased glucose uptake with a standard uptake value (SUV_{max}) of greater than 2.5 as a reference indicating malignancy [25]. A progressive change in size and number of a lesion or an increase of pathological tracer uptake in nonresponders to applied therapy (alternatively a decrease in responders) were considered as hard criteria for malignancy on follow-up examinations. Focal masses were counted lesion-by-lesion. In the case of diffuse infiltration patterns, especially in metastatic disease to the bone, an evaluation system of anatomical regions was applied and lesions were counted

Table 3 Overview of diagnostic accuracy, sensitivity and specificity for the detection of colorectal tumour recurrence in 24 patients examined with FDG-PET-CT and WB-MRI

	PET	WB-MRI
Total lesions confirmed	*n*=162	
Malignant	*n*=77	
Benign	*n*=85	
Local recurrence	*n*=2	*n*=2
False-positive	*n*=1	*n*=0
Lymph nodes	*n*=76	
Malignant	*n*=29	
Benign	*n*=47	
Sensitivity	93% (27/29)	63% (18/29)
Specificity	100% (47/47)	92% (43/47)
Accuracy	97% (74/76)	80% (61/76)
Distant lesions	*n*=83	
Malignant	*n*=46	
Benign	*n*=37	
Sensitivity	80% (37/46)	78% (36/46)
Specificity	95% (35/37)	95% (35/37)
Accuracy	87% (72/83)	86% (71/83)
Overall		
Sensitivity	86% (66/77)	72% (56/77)
Specificity	96% (82/85)	93% (79/85)
Accuracy	91% (148/162)	83% (135/162)

Overall 162 confirmed foci were detected by both investigations

by the bone region affected. In the case of disseminated metastatic disease to the liver or lungs, the degree of metastatic spread was described by affected lung lobes and liver segments, respectively.

All detected lesions, including all questionable or discordant findings between both investigations, were cross-checked by radiological or nuclear medicine follow-up studies for at least 5 months (average 11 months, 5–30 months) as a standard of reference. The following studies were performed for surveillance in *n* patients: PET-CT (*n*=12), CT (*n*=10), WB-MRI (*n*=6), MRI (*n*=6), radiographs (*n*=5), abdominal ultrasound (*n*=1). In all patients with multiorgan metastases whole-body imaging was chosen; in patients with single-organ metastases dedicated imaging was orientated on the anatomic site of metastatic involvement. In the case of a supposed local recurrent tumour finding, histological clarification was achieved.

Statistical analysis

To assess the diagnostic accuracy of both investigations, sensitivities and specificities were calculated for the described lesions. All lesions found with WB-MRI located outside of the overlapping FOV of both investigations (skull base to the proximal femurs) were excluded from calculation of diagnostic accuracy and counted as additional findings. Concordance for the assessment between MRI and PET-CT imaging was calculated. Statistical analyses were performed with SPSS for Windows (Version 15.0, SPSS Inc., Chicago, Illinois)

Results

On a patient-based analysis tumour recurrence was found in 17 of 24 patients (71%), 4 of whom showed unifocal and 13 multifocal disease. One patient was considered free of tumour recurrence by both WB-MRI and PET-CT, but showed rapid progressive lung metastases in 1 month follow-up. Six patients had no visible malignant lesions and also were negative on follow-up examinations.

Altogether PET-CT and WB-MRI detected 162 foci with 77 lesions classified as malignant and 85 lesions considered benign. The correlation between both investigations was 75% (58/77) for the detected malignant lesions. All 19 discordant findings were unequivocally classified by follow-up examinations.

FDG-PET-CT showed an overall diagnostic accuracy of 91% (148/162) with a sensitivity of 86% (66/77) and a specificity of 96% (82/85). WB-MRI altogether achieved

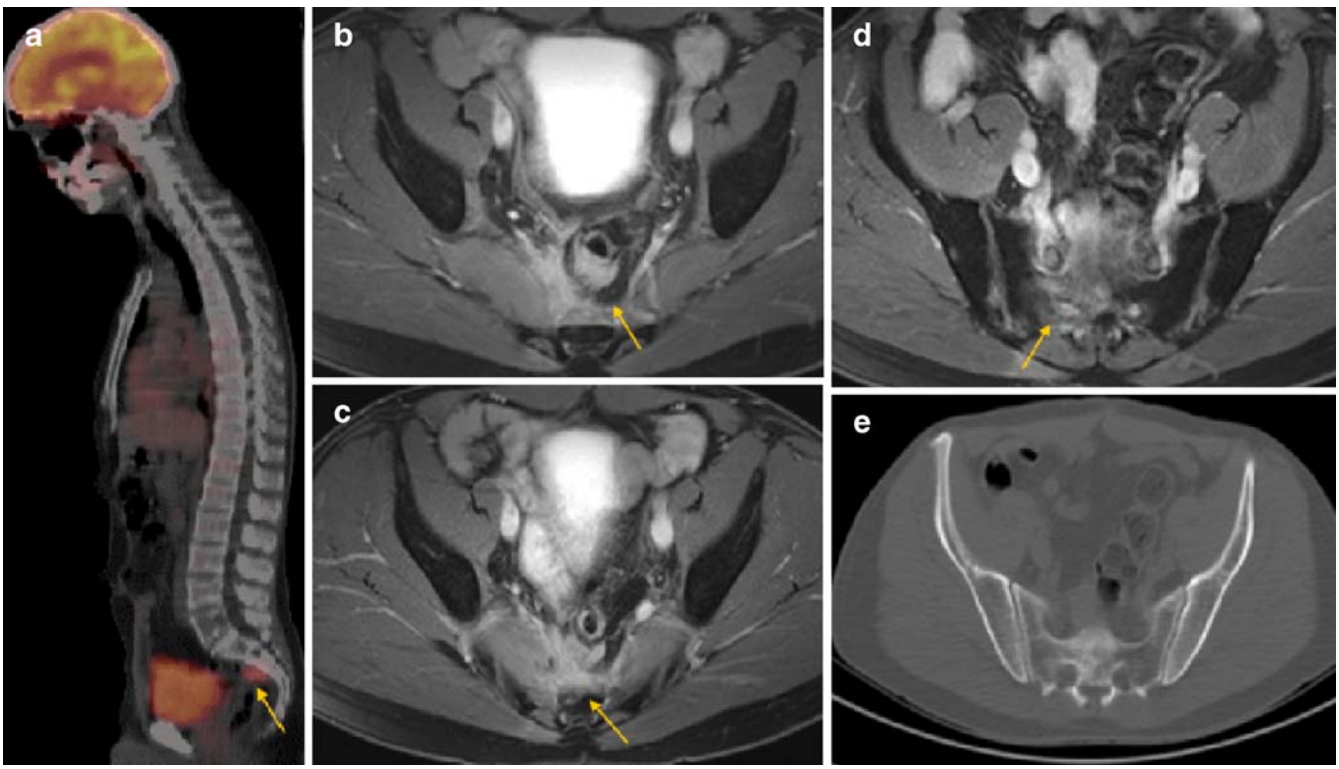

Fig. 1 A 52-year-old male patient with local tumour recurrence. **a** Sagittal PET-CT shows a presacral lesion with increased FDG uptake (SUV_{max} 4.7). **b**,**c** Axial fat saturated 3D-VIBE of the pelvis describes an enhancing mass in the dorsal portion of the rectum with extension into surrounding soft tissue. **d** Furthermore, the beginning of infiltration into the sacral bone is detected. **e** Bone infiltration is undetected in the MS-CT data

an overall diagnostic accuracy of 83% (135/162) with a sensitivity of 72% (56/77) and specificity of 93% (79/85). An overview of calculated diagnostic performance is provided in Table 3.

Local tumour recurrence was detected in two patients by both WB-MRI and PET-CT, more precisely one recurrence of sigmoid cancer and one recurrence of rectal cancer (Fig. 1). Also, one false-positive local tumour recurrence in the right colonic flexure was indicated by PET-CT (Fig. 2). No signs of tumour recurrence were found on WB-MRI and 4- or 10-month PET-CT follow-up in this patient

PET-CT detected significantly more lymph node metastases (sensitivity 93%, 27/29) than WB-MRI (sensitivity 63%,18/29); specificity was 100% (47/47) for PET-CT and 92% for WB-MRI (43/47); diagnostic accuracy was accordingly 97% (74/76) and 80% (71/76). PET-CT particularly detected more lymph node metastases in the hilar/mediastinal region (PET-CT $n=13$ versus WB-MRI $n=6$, Table 4, Fig. 3).

For the detection of distant metastatic disease PET-CT demonstrated a sensitivity of 80% (37/46), WB-MRI 78% (36/46). Specificity was 95% (35/37) for both investigations; diagnostic accuracy was accordingly 87% (72/83) and 86% (71/83). PET-CT revealed more lung metastases (PET-CT $n=12$, WB-MRI $n=8$) and was more sensitive in detecting peritoneal spread (PET-CT $n=2$, WB-MRI $n=0$). Alternatively, WB-MRI revealed more metastases of the bone (WB-MRI $n=4$ versus PET-CT $n=2$) and liver ($n=21$ versus $n=18$, see Table 4, Fig. 4).

Considering the full field of view of a WB-MRI examination, covering the body from head to the calves, additional metastatic disease to the brain was found in one patient.

Examination time for PET-CT was 103 min (60-min patient preparation, imaging time 43 min). Total acquisition time for WB-MRI at 1.5 T was 51:49 min. At 3 T, total acquisition time for WB-MRI was reduced to 42:48 min at identical image resolution. Adding the time for axial STIR imaging of the lung additionally performed at 1.5 T (1:01 min) overall MR data acquisition time at 3 T is reduced by 8:00 min. Mean room time was 61 min at 1.5 T and 52 min at 3 T.

Discussion

Despite a high prevalence of recurrent disease among patients suffering from colorectal cancer, both local tumour

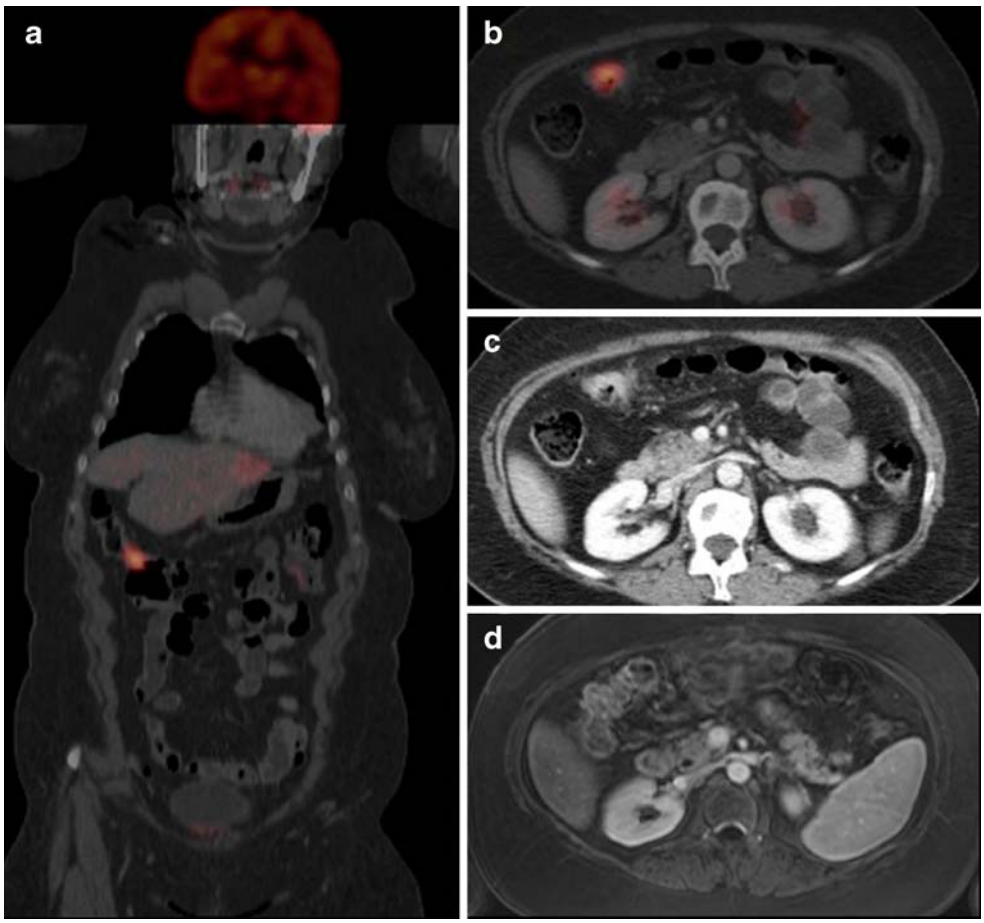

Fig. 2 A 69-year-old woman post sigmoid cancer. **a**,**b** Coronal and axial FDG-PET-CT indicates a distinctive focal tracer uptake (SUV_{max} 6.1) in the proximal segment of the transverse colon. **c** MS-CT shows a correlating semicircular wall thickening suggestive of a tumour recurrence/secondary tumour. **d** Neither WB-MRI correlation in the same segment with use of contrast-enhanced axial VIBE nor 4- and 10-month follow-up with PET-CT confirms the finding

Table 4 Summary of malignant lesions detected by WB-MRI and FDG-PET-CT and anatomical distribution

Malignant lesions	PET-CT	WB-MRI
Local recurrence	2	2
Malignant lymph nodes	27	18
Mesenteric/abdominal	8	7
Paravascular	5	5
Retrocural	1	0
Hilar/mediastinal	13	6
Organ metastases	37	36
Bone	2	4
Liver	18	21
Lung	12	8
Peritoneal carcinosis	2	0
Other	3	3
Total	66	56

Overall 77 malignant foci were detected by both investigations with a correlation of 75%

recurrence and limited metastatic disease can successfully be addressed by curative-intent surgery or intervention with significantly increased survival rates [4–6]. Furthermore, new promising concepts have recently been developed for the therapy of multifocal metastasized colorectal cancer, like selective internal radiation therapy (SIRT), indicating an improvement in patients' progression-free survival [26]. Therefore, an early diagnosis and accurate restaging of recurrent colorectal cancer is important to define appropriate therapeutic strategies.

The basic imaging strategy in the follow-up of patients with colorectal cancer in clinical routine to date mainly consists of a multimodal imaging approach, the standard assessment being multislice CT of the thorax and abdomen. Unfortunately, this approach may also comprise further examinations with either a strong examiner-dependent variation of sensitivity (e.g. abdominal ultrasound) or procedures with limited specificity (e.g. bone scintigraphy for clarification of suspected bone metastases) [21, 27]. Against this background, whole-body imaging investigations such as PET-CT or whole-body MRI are introduced as new promising tools to detect tumour recurrence with high accuracy in its initial stage.

Several studies have described FDG-PET-CT as an effective imaging strategy for restaging of colorectal cancer, improving lesion detection and characterization compared with both PET and CT as standalone investigations, with a reported sensitivity of 89–98% and specificity 83–96% [9, 10, 28, 29]. In this study we assessed WB-MRI as a new whole-body imaging alternative for restaging of colorectal cancer without use of ionizing radiation.

In our study we found a significant patient-based prevalence of recurrent disease of 71%, for the greater part manifesting as multifocal disease (13/17 patients). Only in one patient (with additional hepatic metastases) was early tumour manifestation in the lung falsely interpreted as benign nodules by both PET-CT and WB-MRI at initial presentation. However, these lesions were very small in size (<4 mm), only just visible by WB-MRI, showed partial calcification in CT as well as absent FDG uptake on PET and therefore were difficult to interpret. Limited assessment and impaired diagnostic accuracy of lung nodules below 6 mm in both CT (69%) or MRI (43%) and a reduced sensitivity of PET for small-sized lung lesions has been previously described in the literature [30–32]. As a result of breathing-induced movement of lung parenchyma and depending on the resolution of the PET component, FDG activity can often be underestimated in small lung metastases or show no uptake at all. It has been reported that PET-CT protocols including an additional low-dose CT acquisition of the thorax in expiration phase may enhance sensitivity for lesions smaller than 8 mm, yet clinical relevance of such modified protocols remains unclear [33].

In another patient a false-positive tumour recurrence/secondary tumour was indicated by PET-CT in the right colon flexure, showing no signs of recurrence in WB-MRI correlation and follow-up examinations. Physiological FDG accumulation in the gastrointestinal tract is frequently seen on PET-CT and usually can be differentiated on coronal images due to the linear uptake pattern in bowel mucosa and muscle. Yet, in areas of focal bowel collapse or inadequate distension, bowel uptake may mimic a suspicious mass with circumscribed tracer accumulation, as obviously happened in this patient. To a large extent bowel artefacts at PET can be minimized by administration of *N*-butylscopolamine as recently confirmed by Emmott and co-workers [34]. However, in the case of an ambiguous

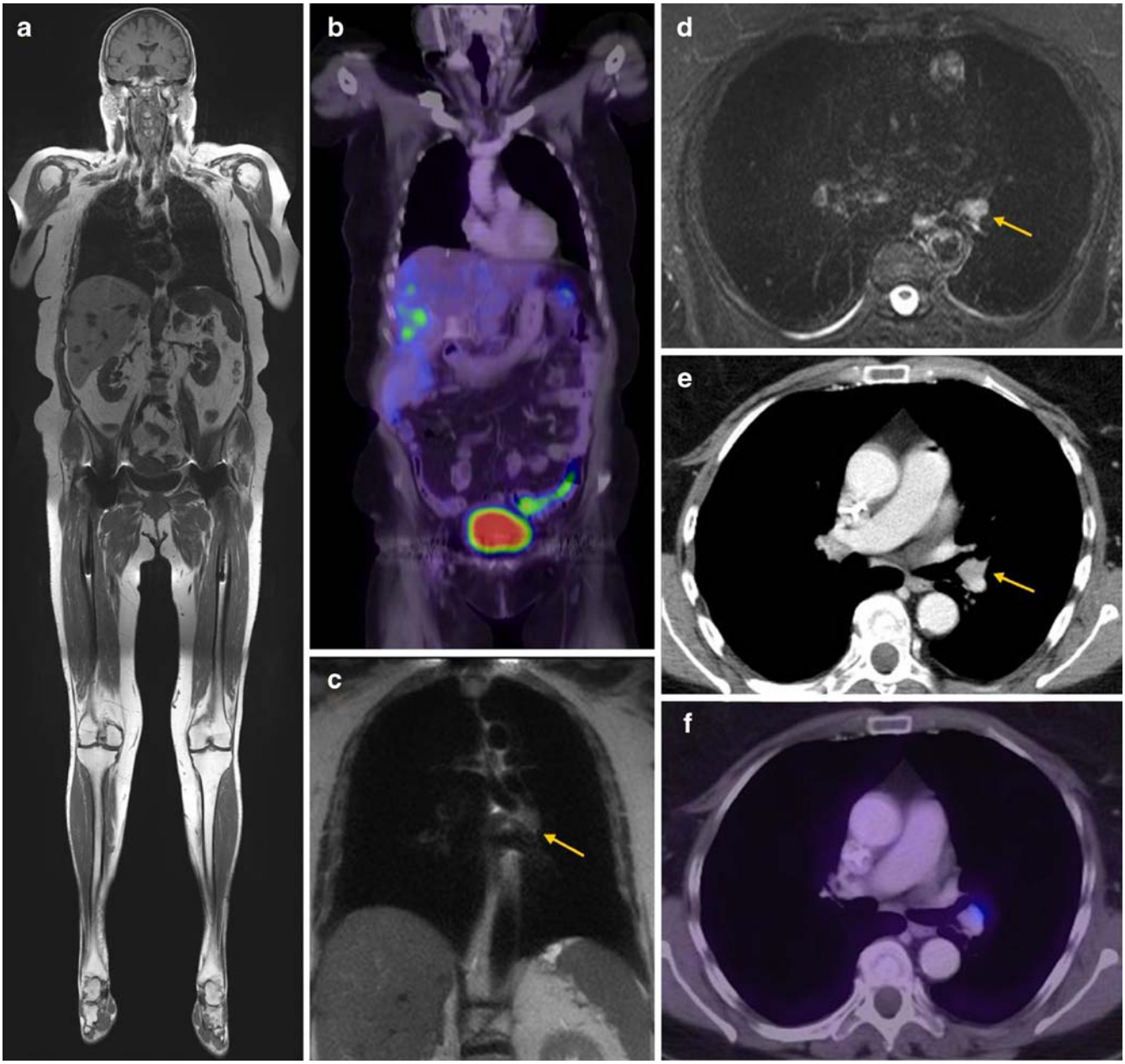

Fig. 3 An 80-year-old patient post cancer of the cecum. **a**,**b** T1w-TSE-WB-MRI shows multiple hypointense liver lesions with a strong FDG uptake (SUV_{max} 5.0) in the PET-CT exam consistent with multifocal liver metastases. **c**,**d** Coronal HASTE of the thorax shows a circumscribed, hypointense soft tissue structure in the left hilar region with hyperintense signal in axial STIR. However, the lesion is difficult to separate from vessel structures with a similar signal and was not described as pathologic in WB-MRI. **e** MS-CT confirms a soft tissue mass consistent with a lymph node 1 cm in size. **f** PET-CT indicates a lymph node metastasis with strong FDG uptake (SUV_{max} 6.8)

finding, a close follow-up examination is advised or correlation with alternative dedicated imaging methods, such as an MR coloscopy. In some cases, endoscopic colonoscopy with lesion biopsy may be needed if results remain inconclusive.

In this study two local tumour recurrences were reliably detected by both investigations. Various studies have described the additional value of FDG-PET-CT for the detection of local tumour recurrence in colorectal cancer, especially for a reliable differentiation from postoperative scar tissue, compared with MS-CT as a standard restaging procedure. A high diagnostic accuracy of PET-CT for detection of local and pelvic recurrence of 89–93% compared with a previously reported accuracy of 65%

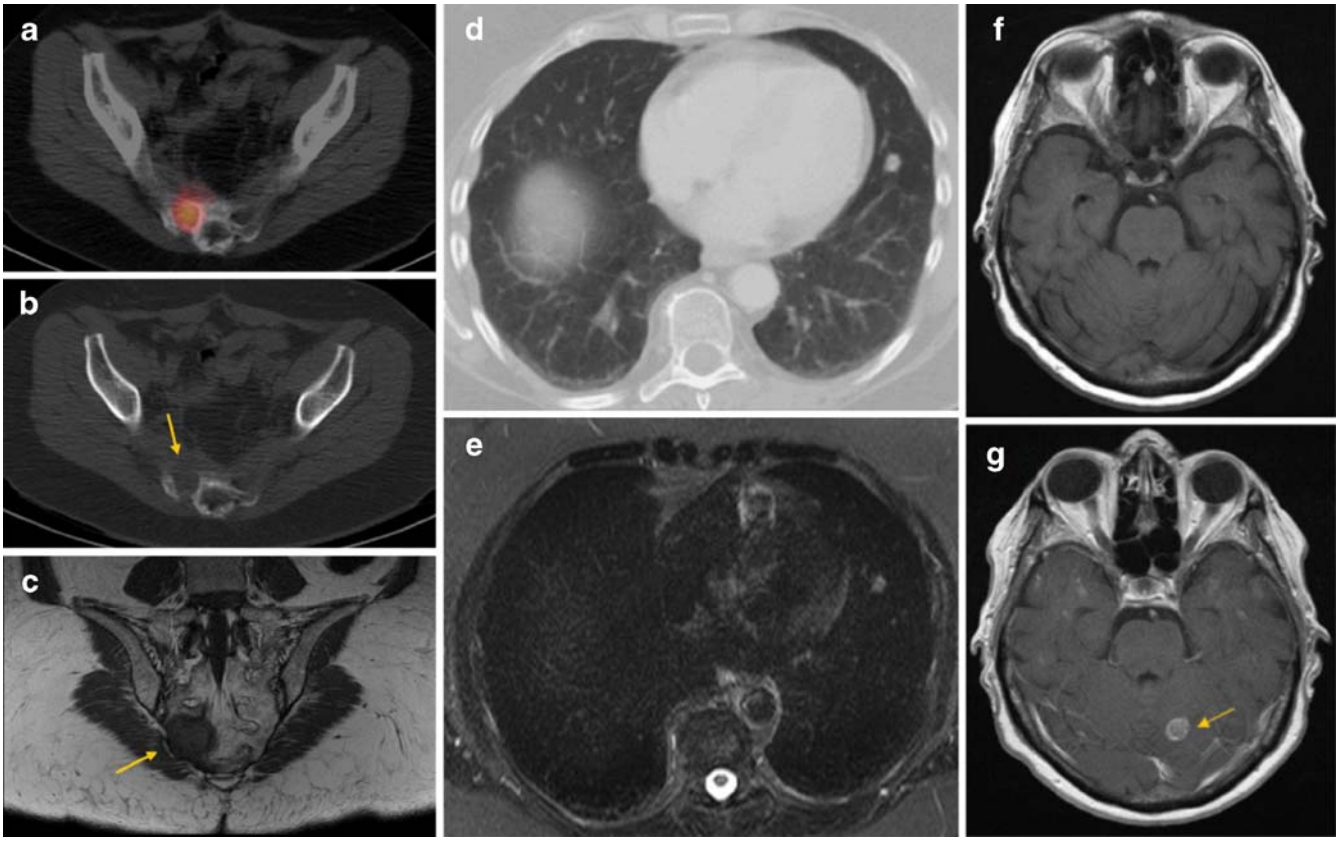

Fig. 4 Whole-body MRI and FDG-PET-CT for the detection of distant metastases. **a**–**c** Bone metastasis in the right sacral bone with avid FDG uptake (SUV_{max} 7.5) in PET-CT and a visible osteolytic defect in MS-CT as well as corresponding hypointense bone lesion in coronal T1-weighted TSE-MRI (*arrows*). **d**,**e** Lung metastasis in a different patient in the left lower lobe, visible in both MS-CT and STIR-MRI at 5-mm size. **f**,**g** Previously unknown brain metastasis in a patient with multifocal disease visible in T1w-WB-MRI pre- and postcontrast. The lesion was not discernable in FDG-PET due to the strong background uptake of the brain using a whole-body approach

achieved by MS-CT alone has been reported [9, 10, 35]. Owing to the high soft tissue contrast in pelvic soft tissue structures MRI is superior to MS-CT for detection of local tumour recurrence with a sensitivity of up to 87% [36, 37]. However, higher located recurrence of colon cancer may require more elaborate imaging approaches, such as MR colonography with adequate bowel preparation, which is difficult to integrate into a clinically sensible WB-MRI approach, focusing on tumour recurrence over the whole-body anatomy.

Both FDG-PET-CT and WB-MRI showed a persuasive overall diagnostic accuracy (PET-CT 91% versus WB-MRI 83%) for lesion-by-lesion detection of tumour recurrence, with a better overall performance indicated by PET-CT. Previous studies have demonstrated the efficacy of both PET-CT and WB-MRI in cancer restaging, yet mainly analysing heterogeneous tumour cohorts as preliminary results [16, 17, 38].

Only one very recently published study, conducted by Squillaci and co-workers, has described WB-MRI in direct comparison to FDG-PET-CT as restaging strategies for colorectal cancer [39]. In their study our observation of a superior performance of FDG-PET-CT over WB-MRI is confirmed, particularly due to a higher sensitivity for the detection of lymph node metastases: Iymph node status was correctly classified as N-positive in 10 of 20 cases by WB-MRI and 15 of 20 cases by PET-CT. We similarly observed a higher diagnostic sensitivity of 93% for PET-CT compared with 63% for WB-MRI. Especially in anatomical regions which are prone to potential artefacts in MRI, such as the retrocural region, the mediastinum or paravascular structures (where image quality may be affected by pulsation artefacts or magnetic susceptibility), suspicious lymph nodes may potentially be missed in a WB-MRI exam. Indeed, our study results show that only six malignant nodes, located either retrocrurally or in the mediastinum, were detected by WB-MRI versus 14 nodes detected by FDG-PET-CT. The usefulness of additional metabolic information provided by PET-CT becomes especially apparent for the detection of borderline-sized nodes potentially harboring micrometastases, when compared with morphologic imaging alone. In a recently published study introducing WB-MRI and MS-CT for the staging of lymphoma, the lack of sensitivity for the

detection of small lymph node metastases (<12 mm) became evident with a reported decline of sensitivity for WB-MRI from 92% down to 67% [40]. A promising concept to enhance diagnostic accuracy for malignant lymph node detection is the STIR-EPI diffusion sequence with adequate fat suppression (DWIBS) [41]. Muertz et al. recently showed the feasibility of this technique as a whole-body application under high field conditions with diagnostic image quality [42]. They described a good correlation for lymph node metastases as depicted by DWIBS and those visualized by FDG-PET. Despite these encouraging reports, this method is still the subject of research and large patient cohort studies have to prove its efficacy in a clinical setting. In particular, the calculated ADC values for whole-body diffusion applications so far have not been shown to ensure a reliable differentiation between benign and malignant nodes in recent clinical trials [43].

Owing to an excellent contrast in soft tissue and parenchymal structures, the main application for WB-MRI is detection of distant metastatic disease, especially in abdominal organs, the brain and bone, which represent frequent metastatic routes in colorectal cancer. Here, both investigations performed very reliably with a comparably high accuracy of 86% for WB-MRI versus 87% for PET-CT. A similar trend has been reported in an initial study for tumour staging performed by Antoch and co-workers with a diagnostic accuracy for the correct assessment of M-stage of 93% and 94%, respectively [10, 38]. In the current study WB-MRI more reliably detected bone metastases (n=4 versus n=2) and liver metastases (n=21 versus n=18), similar to the observations made by the Antoch group for these sites. In particular, the combination of noncontrasted T1-weighted TSE and fat suppressed STIR imaging, as used in our present protocol, has proved to be highly accurate for the discrimination of malignant and benign bone marrow lesions [44]. In some cases, sensitivity of PET-CT can be impaired for smaller bone lesions showing no visible morphologic changes in CT or significant tracer uptake, especially for lesions below double the size of the spatial resolution of PET (which usually is 5 mm). An excellent depiction of liver lesions has been reported for multiphase contrast-enhanced 3D-GRE sequences of the abdomen (VIBE) with a better performance, especially for small-sized lesions, compared with FDG-PET-CT [45, 46]. On the other hand, FDG-PET-CT showed an expected better performance for the detection of lung metastases (n=8 versus n=12) and peritoneal implants (n=2 versus n=0). Yet, fast HASTE imaging in combination with PAT has significantly decreased artefacts in lung MRI and proved highly efficient for the detection of even smaller lung lesions [47]. Recently, the efficient implementation of coronal and axial STIR imaging of the lung in combination with axial HASTE (as used in our protocol) within a WB-MRI approach has been described for the detection of pulmonary lesions, compared with MS-CT as a gold standard modality [48].

WB-MRI with its larger anatomical coverage compared with PET-CT revealed an additional finding of a previously unknown brain metastasis in one patient. As a result of the high FDG uptake of the CNS in the PET examination, cerebral lesions can easily be missed in a whole-body FDG-PET-CT exam. Schlemmer et al. reported similar findings with a comparable protocol on the same multi-channel MR system at 1.5 T. A considerable number of additional diagnoses, like unknown cerebral tumour spread and soft tissue metastases, were made compared with MS-CT as the standard staging method. This led to a change of therapy in 6 of 63 patients (10%) [16].

Total MR acquisition time for WB-MRI including various soft tissue contrast, image orientation and contrast media dynamics at 1.5 T was 51:45 min and exams were tolerated well by all patients. Making use of the increased SNR and keeping identical resolution parameters, acquisition time could even be further reduced down to 43:49 min at 3 T and no SAR-related patient discomfort was reported, thus supporting the introduction of WB-MRI as a clinically feasible application for high field conditions. Several modifications on image parameters described in the methods section had to be performed to adapt the WB-MRI concept to high field conditions. In a preclinical step of platform migration our study group analysed image quality criteria and artefacts between 1.5 T and 3 T for the proposed protocol on 15 healthy volunteers by using the same sequence and resolution parameters [49]. Results showed a comparably good performance on both scanners with only slightly increased artefacts at 3 T, without restraining influence on image quality.

A limiting aspect of this study was that unchanged resolution parameters for WB-MRI (in order to trade SNR for further examination time reduction) did not allow us to analyse effects of an enhanced spatial resolution at 3 T on diagnostic accuracy. In particular, a comparison of lesion-based diagnostic performance between both MR systems was not possible due to unbalanced sample numbers and differing patient subgroups, which were not matched for lesion type and lesion occurrence. Furthermore, the lack of a histological proof as a true gold standard for the detected lesions and verification based on radiological follow-up alone represents another limiting aspect with a remaining potential risk of false-positive findings in benign conditions, such as inflammation for example. On the other hand, as with numerous studies of similar design, obtaining multiple biopsies for tissue verification would have been impracticable and ethically unacceptable [13, 15, 16, 40, 44]. Also, the nonuniform follow-up algorithm represents a limitation compared with a randomized approach for lesion verification. Finally, larger patient cohorts will certainly be necessary to confirm the results described in this initial analysis.

In summary, the robust performance of WB-MRI and PET-CT may significantly improve diagnostic accuracy in colorectal cancer patients with suspected tumour recur-

rence and represent a promising alternative to numerous separate investigations. As a consequence patients might benefit from earlier and more accurate tumour detection and improved therapeutic options. Although PET-CT showed the better overall diagnostic performance and has clear advantages in the assessment of lymph node detection, WB-MRI represents a useful radiation-free alternative, especially in younger, fertile patients with repeated examinations and patients with suspected tumour recurrence in specific organs, such as the brain, liver or bone. Finally, WB-MRI under high field conditions is clinically feasible with reduced examination time. Whether trading of SNR for further resolution enhancement at 3 T will have a positive impact on diagnostic accuracy has yet to be determined.

References

1. World Health Organization (2008) Fact sheet no 297 on worldwide cancer. http://www.who.int/mediacentre/factsheets/fs297/en/index.html Accessed 6 Aug 2008
2. Abir F, Alva S, Longo WE et al (2006) The postoperative surveillance of patients with colon cancer and rectal cancer. Am J Surg 192:100–108
3. Desch CE, Benson AB, Somerfield MR et al (2005) Colorectal cancer surveillance: 2005 update of an American Society of Clinical Oncology practice guideline. J Clin Oncol 23:8512–8519
4. Arriola E, Navarro M, Pares D et al (2006) Imaging techniques contribute to increased surgical rescue of relapse in the follow-up of colorectal cancer. Dis Colon Rectum 49:478–484
5. Vigano L, Ferrero A, Lo Tesoriere, Capussotti L (2008) Liver surgery for colorectal metastases: results after 10 years of follow-up. Long-term survivors, late recurrences, and prognostic role of morbidity. Ann Surg Oncol 15:2458–2464. doi:10.1245/s10434-008-9935-9
6. Gilliams AR, Lees WR (2008) Five-year survival following radiofrequency ablation of small, solitary, hepatic colorectal metastases. J Vasc Interv Radiol 19:712–717
7. Pelosi E, Messa C, Sironi S, Picchio M, Landoni C, Bettinardi V et al (2004) Value of integrated PET/CT for lesion localisation in cancer patients: a comparative study. Eur J Nucl Med Mol Imaging 31:932–939
8. Cohade C, Osman M, Leal J, Wahl RL (2003) Direct comparison of 18F-FDG-PET and PET-CT in patients with colorectal carcinoma. J Nucl Med 44:1797–803
9. Even-Sapir E, Parag Y, Lerman H et al (2004) Detection of recurrence in patients with rectal cancer: PET/CT after abdominoperineal or anterior resection. Radiology 232:815–822
10. Kinner S, Antoch G, Bokisch A, Veit-Haibach P (2007) Whole-body PET/CT-colonography: a possible new concept for colorectal cancer staging. Abdom Imaging 32:606–612
11. Selzner M, Hany TF, Wildbrett P, McCormack L, Kadry Z, Clavien PA (2004) Does the novel PET/CT imaging modality impact on the treatment of patients with metastatic colorectal cancer of the liver. Ann Surg 240:1027–1034
12. Lauenstein TC, Goehde SC, Herborn CU, Goyen M, Oberhoff C, Debatin JF (2004) Whole-body MR imaging: evaluation of patients for metastases. Radiology 233:139–48
13. Schmidt GP, Schoenberg SO, Schmid R, Stahl R, Tiling R, Becker CR et al (2006) Screening for bone metastases: whole-body MRI using a 32-channel system versus dual-modality PET-CT. Eur Radiol 17:939–949
14. Thomson V, Pialat JB, Gay F, Coulon A, Voloch A, Granier A et al (2008) Whole-body MRI for metastases screening: a preliminary study using 3D VIBE sequences with automatic subtraction between non-contrast and contrast enhanced images. Am J Clin Oncol 31:285–292
15. Schlemmer HP, Schäfer J, Pfannenberg C, Radny P, Korchidi S, Müller-Horvat C (2005) Fast whole-body assessment of metastatic disease using a novel magnetic resonance imaging system: initial experiences. Invest Radiol 40:64–71
16. Schmidt GP, Baur-Melnyk A, Herzog P, Schmid R, Tiling R, Reiser MF et al (2005) High-resolution whole-body MRI tumor staging with the use of parallel imaging versus dual modality PET-CT: experience on a 32-channel system. Invest Radiol 40:743–753
17. Fink C, Puderbach M, Biederer J, Fabel M, Dietrich O, Kauczor HU (2007) Lung MRI at 1.5 and 3 Tesla: observer preference study and lesion contrast using five different pulse sequences. Invest Radiol 42:377–383
18. Schmidt GP, Wintersperger B, Graser A, Baur-Melnyk A, Reiser MF, Schoenberg SO (2007) High-resolution whole-body magnetic resonance imaging applications at 1.5 and 3 Tesla: a comparative study. Invest Radiol:449-459
19. Hargreaves BA, Cunningham CA, Nishimura DG, Conolly SM (2004) Variable rate selective excitation for rapid MRI sequences. J Magn Reson Med 52:590–597
20. Stehling G, Niederstadt T, Kramer S, Kugel H, Schwindt W, Heindel W et al (2005) Comparison of a T1-weighted inversion recovery-, gradient echo- and spin-echo sequence for imaging of the brain at 3.0 Tesla. Fortschr Roentgenstr 177:536–542
21. Engelhard K, Hollenbach HP, Wohlfart K, von Imhoff E, Fellner FA (2004) Comparison of whole-body MRI with automatic moving table technique and bone scintigraphy for screening for bone metastases in patients with breast cancer. Eur Radiol 14:99–105
22. Brix G, Lechel U, Glatting G, Ziegler SI, Muenzing W, Mueller SP et al (2005) Radiation exposure of patients undergoing whole-body dual-modality 18F-FDG-PET/CT examinations. J Nucl Med 46:608-613
23. Vanel D, Bittoun J, Tardivon A (1998) MRI of bone metastases. Eur Radiol 8:1345–1351
24. Danet IM, Semelka RC, Leonardou P, Braga L, Vaidean G, Woosley JT et al (2003) Spectrum of MRI appearances of untreated metastases of the liver. Am J Roentgenol 181:809–817
25. Beggs AD, Hain SF, Curran KM, O'Doherty MJ (2002) FDG-PET as a "metabolic biopsy" tool in non-lung lesions with indeterminate biopsy. Eur J Nucl Med Mol Imaging 29:542–546

26. Welsh JS, Kennedy AS, Thomadsen B (2006) Selective internal radiation therapy (SIRT) for liver metastases secondary to colorectal adenocarcinoma. Int J Radiat Oncol Biol Phys 66: S62–S73
27. Curati WL, Halevy A, Gibson RN, Carr DH, Blumgart LH, Steiner RE (1988) Ultrasound, CT and MRI comparison in primary and secondary tumors of the liver. Gastrointest Radiol 13:121–123
28. Chen LB, Tong JL, Song HZ, Zhu H, Wang YC (2007) (18)F-DG PET/CT in detection of recurrence and metastasis of colorectal cancer. World J Gastroenterol 13:5025–5029
29. Votrubova J, Belohlavek O, Jaruskova M, Oliverius M, Lohynska R, Trskova K et al (2006) The role of FDG-PET/CT in the detection of recurrent colorectal cancer. Eur J Nucl Med Mol Imaging 33:779–784
30. Diederich S, Semik M, Lentschig MG, Winter F, Scheld HH, Roos N et al (1999) Helical CT of pulmonary nodules in patients with extrathoracic malignancy: CT-surgical correlation. Am J Roentgenol 172:353–360
31. Frericks BB, Meyer BC, Martus P, Wendt M, Wolf KJ, Wacker F (2008) MRI of the thorax during whole-body MRI: evaluation of different MR sequences and comparison to thoracic multi-detector computed tomography (MDCT). J Magn Reson Med:538-545
32. Bruegel M, Gaa J, Woertler K, Ganter C, Waldt S, Hillerer C, Rummeny EJ (2007) MRI of the lung: value of different turbo spin-echo, single-shot turbo spin-echo, and 3D gradient-echo pulse sequences for the detection of pulmonary metastases. J Magn Reson Imaging 25:73–81
33. Juergens KU, Weckesser M, Stegger L, Franzius C, Beetz M, Schober O et al (2006) Tumor staging using whole-body high-resolution 16-channel PET-CT: does additional low-dose chest CT in inspiration improve the detection of solitary pulmonary nodules. Eur Radiol 16:1131–1137
34. Emmott J, Sanghera B, Chambers J, Wong WL (2008) The effects of N-butylscopolamine on bowel uptake: an 18F-FDG PET study. Nucl Med Commun 29:11–16
35. Schiepers C, Pennickx F, de Vadder N, Merckx E, Mortlemans L, Bormans G et al (1995) Contribution of PET in the diagnosis of recurrent colorectal cancer: comparison with conventional imaging. Eur J Surg Oncol 21:517–522
36. Dicle O, Obuz F, Cakmakci H (1999) Differentiation of recurrent rectal cancer and scarring with dynamic MR imaging. Br J Radiol 72:1155–1159
37. Titu LV, Nicholson AA, Hartley JE et al (2006) Routine follow-up by magnetic resonance imaging does not improve detection of resectable local recurrences from colorectal cancer. Ann Surg 243:348–352
38. Antoch G, Vogt FM, Freudenberg LS, Nazaradeh F, Goehde SC, Barkhausen J et al (2003) Whole-body dual-modality PET/CT and whole-body MRI for tumor staging in oncology. JAMA 290:3199–3206
39. Squillaci E, Manenti G, Mancino S, Ciccio C, Calabria F, Danieli R et al (2008) Staging of colon cancer: whole-body MRI vs whole-body PET-CT-initial clinical experience. Abdom Imaging 33:676–688. doi:10.1007/s00261-007-9347-5
40. Brennan DD, Gleeson T, Coate LE, Cronin C, Carney D, Eustace SJ (2005) A comparison of whole-body MRI and CT for the staging of lymphoma. AJR 185:711–716
41. Takahara T, Imay Y, Yamashita T, Yasuda S, Nasu S, Van Cauteren M (2004) Diffusion weighted whole body imaging with background body signal suppression (DWIBS): technical improvement using free breathing, STIR and high resolution 3D display. Radiat Med 22:275–282
42. Muertz P, Krautmacher C, Traeber F, Gieseke J, Schild HH, Willinek WA (2007) Diffusion-weighted whole-body MR imaging with background body signal suppression: a feasibility study at 3.0 Tesla. Eur Radiol 17(12):3031–3037
43. Lichy MP, Aschoff P, Plathow C, Stemmer A, Horger W, Mueller-Horvath C et al (2007) Tumor detection by diffusion-weighted MRI and ADC-mapping—initial clinical experiences in comparison to PET-CT. Invest Radiol 42:605–613
44. Mehta RC, Marks MP, Hinks RS, Glover GH, Enzmann DR (1995) MR evaluation of vertebral metastases: T1-weighted short inversion time inversion recovery, fast spin echo, and inversion-recovery fast spin-echo sequences. Am J Neuroradiol 16:281–288
45. Semelka RC, Martin DR, Balci C, Lance T (2001) Focal liver lesions: comparison of dual-phase CT and multi-sequence multi-planar MR imaging including dynamic gadolinium enhancement. J Magn Reson Imaging 13:397–401
46. Dobritz M, Radkow T, Nittka M, Bautz W, Fellner FA (2002) VIBE with parallel acquisition technique—a novel approach to dynamic contrast-enhanced MR imaging of the liver. Fortschr Roentgenstr 174:738.41
47. Vogt FM, Herborn CU, Hunold P et al (2004) HASTE MRI versus chest radiography in the detection of pulmonary nodules: comparison with MDCT. AJR 183:71–78
48. Frericks BB, Meyer BC, Martus P, Wendt M, Wolf KJ, Wacker F (2008) MRI of the thorax during whole-body MRI: evaluation of different MR sequences and comparison to thoracic multi-detector computed tomography (MDCT). J Magn Reson Imaging 27:538–545
49. Schmidt GP, Wintersperger B, Graser A, Baur-Melnyk A, Reiser MF, Schoenberg SO (2007) High-resolution whole-body magnetic resonance imaging applications at 1.5 and 3 Tesla: a comparative study. Invest Radiol 42:449–459